Properties of $CsCl/AlCl_3$ Melts Near Equimolar Composition and the Problem of Corrosive Action of the Melt towards Container Materials

R. W. Berg,[a] T. L. Lauridsen,[a] T. Østvold,[b] H. A. Hjuler,[a] J. H. von Barner[c] and N. J. Bjerrum[a]

[a]Chemistry Department A, The Technical University of Denmark, DK-2800 Lyngby, Denmark, [b]Institute of Inorganic Chemistry, The University of Trondheim – The Norwegian Institute of Technology, N-7034 Trondheim-NTH, Norway and [c]Institute of Mineral Industry, The Technical University of Denmark, DK-2800 Lyngby, Denmark

Berg, R. W., Lauridsen, T. L., Østvold, T., Hjuler, H. A., Barner, J. H. von and Bjerrum, N. J., 1986. Properties of $CsCl/AlCl_3$ Melts Near Equimolar Composition and the Problem of Corrosive Action of the Melt towards Container Materials. – Acta Chem. Scand. A 40: 646–657.

The phase diagram of the molten salt system $CsCl/AlCl_3$ near the equimolar composition contained in pyrex glass or stainless steel has been studied by cryoscopic methods. A congruent melting point of 387.7 °C was observed for $CsAlCl_4$, some 10 °C higher than given previously. Approximate values and uncertainty ranges of the enthalpy and entropy of freezing and the cryoscopic constant of $CsAlCl_4$ at the melting point were found and are reported. By potentiometric measurements with concentration cells, the solubility at 400 °C of CsCl in the $CsCl/AlCl_3$ melt was determined. Potentiometric results for near neutral and weakly acidic melts (up to $x_{AlCl_3} = 0.53$) could be explained satisfactorily by the equilibrium $2AlCl_4^- \rightleftarrows Al_2Cl_7^- + Cl^-$ with a stoichiometric equilibrium constant equal to $10^{-7.63}$ at 400 °C (molar units), in reasonable agreement with previously published results. The density of $CsCl/AlCl_3$ melts was determined dilatometrically and is described as a function of temperature and composition. The container materials were somewhat attacked by the melts. Thus, although the melts were highly purified, the results obtained relate to slightly impure melts.

Chloroaluminate melts have attracted considerable interest because of their special properties as ionic solvents, for their application in aluminium production, and for their possible use as electrolytes in rechargeable high energy-density batteries. We have previously investigated the properties of $NaCl/AlCl_3$ and $KCl/AlCl_3$ melts near the neutral 1:1 composition by cryoscopy[1,2] and potentiometry.[3,4] In the present paper, the $CsCl/AlCl_3$ system is described.

The phase diagram for the $CsCl/AlCl_3$ system has previously been studied twice.[5,6] CsCl has an $\alpha \rightleftarrows \beta$ phase transformation occurring probably at a temperature of 469 ± 1 °C.[7,8] A two-liquid region in $AlCl_3$-rich melts has been observed[6] up to the critical point of $AlCl_3$, occurring at 348–349 °C.[9] When these results are summarized as in Fig. 1, a satisfactory overall consistency is seen.

Several authors[10–13] have investigated the $CsCl/AlCl_3$ system by means of the potentiometric method, and found evidence for the equilibrium given in eqn. (1) near the equimolar composition. Known values of the equilibrium constant K_1 are given in Table 1.

$$2AlCl_4^- \rightleftarrows Al_2Cl_7^- + Cl^- \qquad (1)$$

To fully understand the cryoscopic data obtained on adding CsCl or $AlCl_3$ to $CsAlCl_4$, a thermodynamic model for the melt is required. In chloroaluminate melts, $MCl/AlCl_3$ (M = Na, K, Cs), the predominant equilibrium near a molar ratio $MCl:AlCl_3 = 1$ is the reaction in eqn. (1), although a fully satisfactory thermodynamic model should also involve small quantities of the $AlCl_3$ and Al_2Cl_6 species and take the effect of the dif-

Table 1. Values of the equilibrium constant K_1, expressed as $pK_1 = -\log K_1$, for eqn. (1) in CsCl/$AlCl_3$ melts.[a]

Refs.	T = 400 °C	T = 450 °C
Torsi and Mamantov[10]	7.4	6.8
Schulze *et al.*[11]	–	6.1
Ikeuchi and Krohn[12]	–	5.48
Berg *et al.*[13]	7.60	–
This work	7.627±0.004[b]	–

[a]K_1 expressed in mole fractions or in concentrations: $x_{Cl^-} \cdot x_{Al_2Cl_7^-}/x^2_{AlCl_4^-} = [Cl^-] \cdot [Al_2Cl_7^-]/[AlCl_4^-]^2$. [b]Standard error from the calculations. The actual error may be larger.

ferent M^+ ions into account, as shown by Øye *et al.*[14-15] The magnitude of K_1 (Table 1) indicates that $AlCl_4^-$ is the predominant ion when the CsCl:$AlCl_3$ ratio is near 1, possibly up to a mole fraction of $AlCl_3$ near 0.55.

Experimental

Chemicals. To keep the chemicals essentially free of moisture, they were handled by standard glove box techniques.[1] CsCl, treated as previously,[16] was recrystallized by zone melting in silica ampules. $AlCl_3$ from Fluka was sublimed and distilled four times in Pyrex ampules. $CsAlCl_4$ obtained by zone refining a 1:1 mixture of CsCl and $AlCl_3$ was used for preparing the samples.

Cryoscopy. The sampling containers (cells) were of two constructions, both equipped with a thermometer pocket for a 100 Ω platinum resistor and designed for sealing under vacuum. The cell material was either Pyrex glass, as previously,[1,2] or NU 3L Stainless and Kovar steels, which made cell fabrication possible by microplasma welding in an argon atmosphere (see Fig. 2). The steel cells were rinsed for oxides in hydrochloric acid (3M), washed in water, vacuum dried at 100 °C, filled with reagents through a long funnel, closed, and finally sealed under vacuum by welding. Prior to the cryoscopic measurements, the samples were homogenized by rocking at 5 °C above the melting point in a multiple-zone tube furnace.

Crystallization was initiated by tempering the cell, mounted in a standardized holder, such that the subcooling was as little as possible.[1] It sometimes proved favorable to make seeds of crystallites at the top of the stem (Fig. 2, A), temper the rest of the cell, and then turn the cell upside down for a moment to initiate crystallization. The resistance thermometer was calibrated at 0, 231.97 and 419.58 °C using pure water, tin (99.999 w %) and zinc (99.99 w %), respectively. The freezing points determined are considered accurate to within 0.1 to 1.0 °C, depending mainly on the mass of the sample in the cell and on the composition.

Further details of the technique are given elsewhere.[1,2]

Potentiometry. The experimental details of this electrochemical method have been described previously in detail,[3,4,17] except for the modifications inherent in Fig. 3 showing the type of chlorine/chloride concentration cell employed. The construction of chloroaluminate/aluminium con-

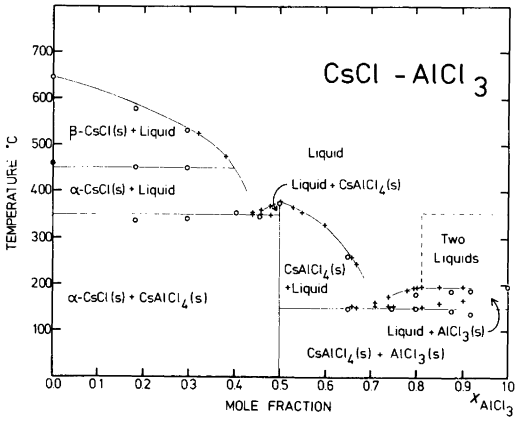

Fig. 1. Phase diagram of the CsCl/$AlCl_3$ system according to the literature (○, +, and ● correspond to Refs. 5, 6 and 7, respectively).

centration cells was similar except that no chlorine was added and the glassy carbon rods were replaced with electrodes of pure aluminium wire in contact with tungsten wire which was sealed vacuum-tight through Pyrex glass. Because of the high temperature (400±0.5 °C), cell tightness around the glassy carbon electrodes could only be achieved with elongated seals, as shown in Fig. 3, K.

Density. The volumes of the $CsCl/AlCl_3$ mixtures were measured in quartz dilatometric cells with two chambers **A** and **B** separated by a (vertical) capillary tube having engraved marks. Calibration of volume **B** was done by filling **B** with water and weighing at 25 °C. After loading with CsCl and $AlCl_3$ salts, the mixture was melted and homogenized horizontally in chamber **A**, then poured into the calibrated **B** chamber. Chamber **A** was sealed off at the capillary and the mass of the mixture corrected for salt remaining in **A**. The position of the melt meniscus in the capillary

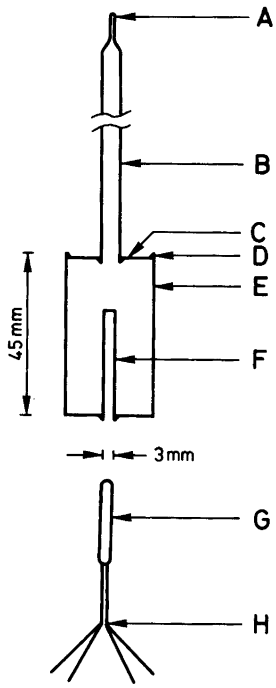

Fig. 2. Cryoscopic cell of NU 3L stainless steel: A, sealing position; B, stem; C, lid of Kovar stainless steel; D, welding; E, container; F, thermometer pocket; G, thermometer; H, leads.

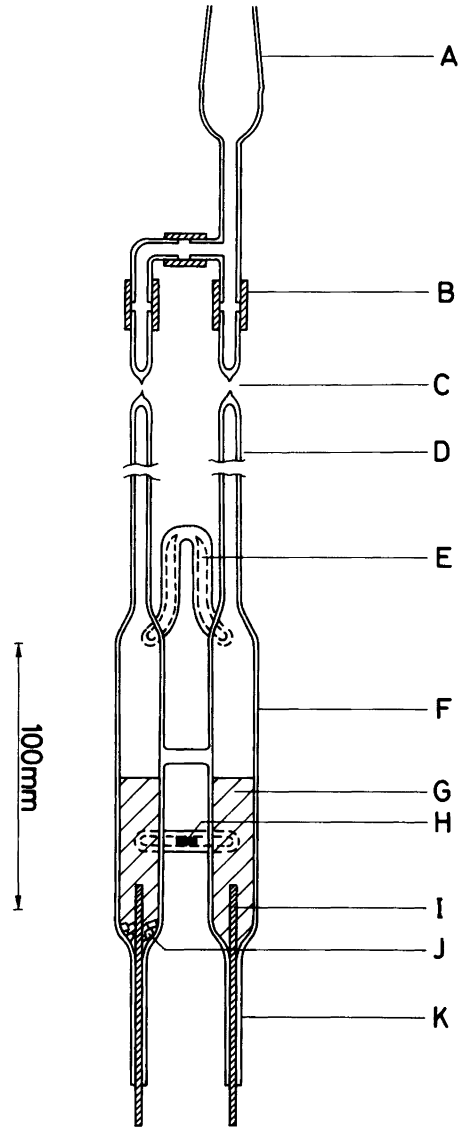

Fig. 3. Potentiometric cell of Pyrex glass: A, joint; B, rubber; C, sealing position; D, stems; E, sealed connecting tube; F, cell compartment; G, melt; H, sintered Pyrex disk of low porosity (resistance 20–80 kΩ when tested with 0.1 M aqueous KCl at room temperature); I, glassy carbon electrode; J, crystals of CsCl; K, elongated lead-through.

was then measured (with an elongated micrometer screw) as a function of temperature in a vertical glass furnace. The precision of the volume

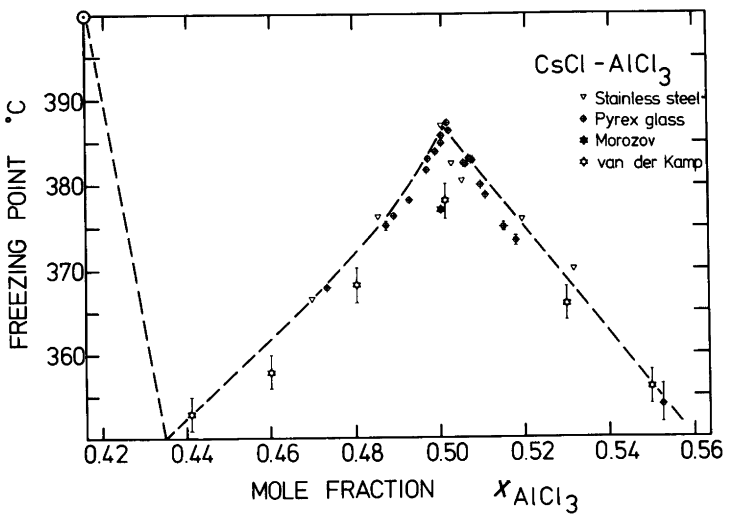

Fig. 4. Refined section of the CsCl/AlCl$_3$ phase diagram, near equimolar composition (Refs. 5, 6 and this work). The dashed curves represent the most likely position of the liquidus curves.

and mass was estimated to be better than 0.2%. The temperature was recorded with a Pt/Pt 10% Rh thermocouple to an accuracy of the order of ±2°C, which might yield 0.4% error in density. The volume was not corrected for the (vanishingly small) expansion of the quartz.

Results and discussion

Phase diagram. Our measurements (Table 2) are shown graphically in Fig. 4, together with previous results.[5,6] It is seen that our freezing points near the equimolar composition are much higher than those previously found. This is presumably due to impurities in the reagents used by the other workers (the AlCl$_3$ *pro analysi* in Ref. 6 had a 4°C melting interval, indicating a significant content of impurities). On fractional recrystallization, the freezing point (of the crystalline fraction) rose to 387.7°C (expts. D, Table 2), and

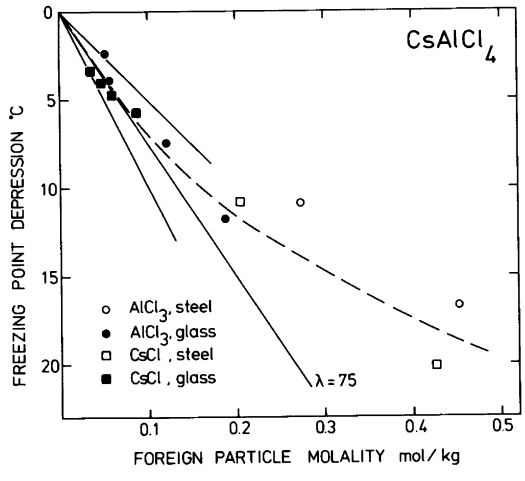

Fig. 5. Freezing point depression, θ, for CsAlCl$_4$ vs. molality *m* of added foreign substances of AlCl$_3$ or CsCl in Pyrex glass or stainless steel cells. Lines corresponding to λ = 75±25°C kg mol^{-1} are shown.

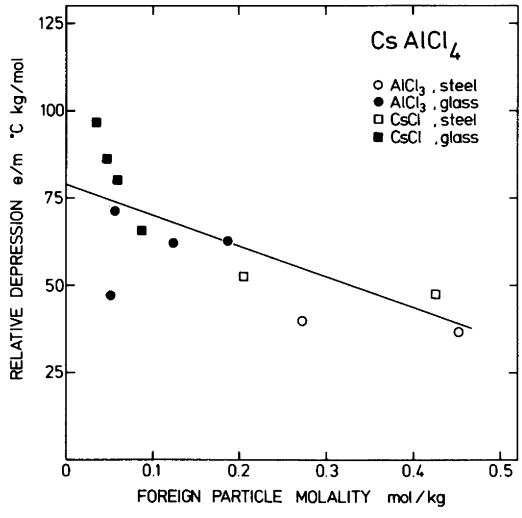

Fig. 6. Relative freezing point depression, θ/*m*, for CsAlCl$_4$ vs. molality *m* of added foreign substances. The line shown is the regression line.

this must be considered as a close approach to the true freezing point.

In contrast to common phase diagram behavior,[18] the congruently melting $CsAlCl_4$ compound does not exhibit an experimental horizontal tangent in the liquidus curve. In our opinion, the presence of a sharp (not rounded) peak at $x_{AlCl_3} = 0.5$ (x = mole fraction determined from weights) indicates that the complex $AlCl_4^-$ is stable and does not self-dissociate appreciably to $Al_2Cl_7^-$ (or $AlCl_3$) and Cl^-, in agreement with previous results, as noted in the introduction.

In the acidic range, evaporation of $AlCl_3$ (or Al_2Cl_6) into the empty volume above the melt was not taken into account when calculating the melt compositions. This would, however, give rise to very small composition errors because of the small (~10 cm^3) empty volumes employed.

The maximum temperature in Fig. 4 obviously does not correspond to exactly $x_{AlCl_3} = 0.5$. This is undoubtedly due to a slight oxide contamination of the $AlCl_3$ used.[1]

As previously with $NaAlCl_4$[1] and $KAlCl_4$,[2] we tried to calculate the solubility of solid CsCl in basic molten $CsCl/AlCl_3$ mixtures, i.e. the CsCl liquidus curve, expressed as x_{AlCl_3} vs. the absolute temperature T. The four known points[5,6] on this curve (see Fig. 1) were used to find the best possible expression, eqn. (2), where A and B are parameters.

$$\log (0.5 - x_{AlCl_3}) = A - \frac{B}{T} \qquad (2)$$

The fit was not good, giving a coefficient of determination[19] $R^2 = 0.9834$, with the values A = 2.5786 and B = 2631. Inclusion of our potentiometrically determined point ($x_{AlCl_3} = 0.4151$ at 400 °C, see below) gave values A = 1.5243, B = 1779.4 and $R^2 = 0.9281$, indicating an even worse fit. The cause of this is presumed to be the occurrence of the CsCl $\alpha \rightleftarrows \beta$ phase transition at ca. 469 °C, which might cause the liquidus curve to change its slope suddenly. In our opinion, the best way to estimate the position of the liquidus was to use our solubility value at 400 °C and the literature data[6] at 475 °C, from which we obtained A = 0.3927, B = 985.5 and hence x_{AlCl_3} (350 °C) = ca. 0.435. From this result, it seems correct to assign the literature point[6] at (x_{AlCl_3}, T) = (0.441, 353 °C) to the $CsAlCl_4$ liquidus. The estimated liquidi are shown as dashed curves in Fig. 4. It is seen that the eutectic point seems to occur at ca. 350 °C for $x_{AlCl_3} = 0.435$. This result is in close agreement with the position (0.443, 350 °C) given in Ref. 6.

Cryoscopy of $CsAlCl_4$. When CsCl is added to $CsAlCl_4$ melts, the Cl^- ion will be the main new species. When $AlCl_3$ is added to the melt, however, both $Al_2Cl_7^-$ and $AlCl_3$ (or Al_2Cl_6) will be present, in addition to the $AlCl_4^-$ species. According to a model by Øye *et al.*,[14,15] which describes the melt as a mixture of Cs^+, Cl^-, $AlCl_4^-$, $Al_2Cl_7^-$, and $AlCl_3$ (Al_2Cl_6) entities, the mole fraction of the $AlCl_3$ (or Al_2Cl_6) molecules is several orders of magnitude lower than that of $Al_2Cl_7^-$ in near neutral melts.

The freezing point depression of $CsAlCl_4$, when adding CsCl or $AlCl_3$, θ, may then be calculated by the Raoult-van't Hoff relation with the assumption that the mixture contains an ideal anion mixture of Cl^- and $AlCl_4^-$ in the basic region, and of $Al_2Cl_7^-$ and $AlCl_4^-$ in the acidic region. This gives eqn. (3), where x_i^{excess} is the mole fraction of excess CsCl or $AlCl_3$ added, defined as in eqn. (4) for the basic case (for the acidic case, CsCl and $AlCl_3$ are permuted; n_i = number of moles of i). ν is the number of moles of new entities formed for each mole of added substance (in the present system $\nu = 1$), R is the gas constant and ΔH_f° is the enthalpy of fusion at T_f, the freezing point of the pure solvent.

$$\theta = \nu x_i^{excess} \frac{RT_f^2}{\Delta H_f^\circ} \qquad (3)$$

$$x_{CsCl}^{excess} \simeq \frac{n_{CsCl} - n_{AlCl_3}}{n_{AlCl_3}} \qquad (4)$$

Using molality m instead of mole fraction x, we obtain eqn. (5).

$$\lambda = \frac{\theta}{\nu m} = \frac{M_{CsAlCl_4}}{1000} \frac{RT_f^2}{\Delta H_f^\circ} \qquad (5)$$

Here λ is the molal freezing point depression constant and M is the molar mass (in °C kg mol^{-1} and g mol^{-1}, respectively). A necessary requirement for ΔH_f° to be the *true* enthalpy of fusion is that the self-dissociation of the $AlCl_4^-$ ion is small.[20]

Determination of the cryoscopic constant, λ. The freezing point depression constant can be estimated from the Raoult-van't Hoff equation, eqn. (5), and the data in Table 2. Useful combinations of experiments are given in Table 3. The reference experiments were chosen as those which had compositions close to $x_{AlCl_3} = 0.5$ and freezing points indicating that melts were essentially pure $CsAlCl_4$. Values of m and θ are plotted in Fig. 5. As discussed above, it is reasonable to assume that $Al_2Cl_7^-$ and Cl^- are the cryoscopically active entities in acidic and basic melts, respectively. The common Cs^+ ions are cryoscopically inactive. Also, for the congruently melting $NaAlCl_4$ and $KAlCl_4$ compounds in the respective NaCl/$AlCl_3$ and KCl/$AlCl_3$ systems, $\nu = 1$ was observed.[1,2] In Fig. 5, similar behavior is seen for $CsAlCl_4$. There is sufficient agreement between θ versus m obtained from both $AlCl_3$ and CsCl additions to indicate that ν is indeed indentical. To determine λ, the slope of the curve in Fig. 5 should be evaluated at $m = 0$. This extrapolation is difficult to make because of the large scatter for small m. Linear regression of all points

Table 2. Observed freezing points T_f as a function of the $AlCl_3$ mole fraction, determined from weights.

Experiment No.	$AlCl_3$/mol	CsCl/mol	x_{AlCl_3}	T_f/°C
Pyrex glass cells				
A–0	0.05640	0.05405	0.51061	378.7
A–1	0.05640	0.05510	0.50581	382.3
A–2	0.05640	0.05600	0.50176	386.2
A–3	0.50640	0.05636	0.50019	384.8
B–0	0.05403	0.05205	0.50932	379.9
B–1	0.05403	0.05283	0.50563	382.3
B–2	0.05403	0.05432	0.49868	383.75
B–3	0.05383	0.05549	0.49240	378.0
B–4	0.05383	0.05630	0.48877	376.1
C–0	0.1203	0.1178	0.5054	382.45
C–1	0.1203	0.1203	0.5000	385.65
C–2	0.1203	0.1220	0.4966	381.6
D–0	0.21356	0.21245	0.50131	387.15
D–1	–	–	–	387.55
D–2	–	–	–	387.75
D–3	–	–	–	387.7
E–0	0.09279	0.07508	0.55274	351.8–356.4[a]
F–0	0.06832	0.07619	0.47277	367.4–367.9[a]
F–1	0.07524	0.07619	0.49686	382.9
F–2	0.07833	0.07619	0.50691	382.75
G–0	0.06827	0.06355	0.51789	373.9
H–0	0.16790	0.17696	0.48686	375.4
I–0	0.11772	0.11089	0.51493	375.4
Steel cells				
S1–0[b]	0.03727	0.03727	0.50000	385.3
S2–0	0.11282	0.09927	0.53195	370.1
S2–1	G.11282	0.10424	0.51976	375.9
S2–2	0.11282	0.11056	0.50505	380.8
S3–0	0.07988	0.09015	0.46978	366.6
S4–0	0.08732	0.08644	0.50252	382.4
S5–0[b]	0.06774	0.06774	0.50000	386.8
S6–0[c]	0.07392	0.07849	0.48501	376.0

[a]Temperature increased with time. [b]Zone-refined $CsAlCl_4$. [c]Zone-refined $CsAlCl_4$+CsCl.

Table 3. Experiments used for estimation of the limiting freezing point depression constant, λ.[a]

Reference expt.	Observation expt.	Addition/ mmol[b]	Solvent amt./ mmol	Molality *m* increment/ mol kg^{-1} of solvent	Depression, θ/ °C[c]	Slope, θ/*m*/ °C kg mol^{-1}
A−2	A−1	0.92	56.00	0.0564 $AlCl_3$	3.9	71.5
A−2	A−0	2.03	56.00	0.1204 $AlCl_3$	7.5	62.3
B−1	B−0	0.81	52.83	0.0508 $AlCl_3$	2.4	47.2
D−0	I−0	11.98	212.45	0.1868 $AlCl_3$	11.75	62.9
B−2	B−3	1.38	54.20	0.0874 CsCl	5.75	65.8
C−1	C−2	1.70	120.30	0.0468 CsCl	4.05	86.4
D−0	B−2	2.26	213.00	0.0352 CsCl	3.40	96.7
D−0	F−1	3.81	213.00	0.0592 CsCl	4.75	80.2
					Average	71.6±16
S5−0	S2−1	8.58	104.24	0.2728 $AlCl_3$	10.9	40.0
S5−0	S2−0	13.55	99.27	0.4524 $AlCl_3$	16.7	36.9
S5−0	S6−0	4.57	73.92	0.2049 CsCl	10.8	52.7
S5−0	S3−0	10.27	79.88	0.4261 CsCl	20.2	47.5
					Average	44.3±7

[a]The selection of data from Table 2 was done to obtain most reliable combinations, e.g. experiment S1−0 was omitted due to the small mass of reagents, S2−2 was a long-time expt. and S4−0 was apparently an outlier. [b]The relative increment in $AlCl_3$ or CsCl was calculated from Table 2. [c]Freezing point depression from reference to observation experiment. See Table 2.

Table 4. Potentiometric results for molten CsCl/$AlCl_3$ at 400 °C.

Expt. No.	Mole fraction x_{AlCl_3}	Potential $-\Delta E$/mV	Y	Chloride excess[a] $C'_{CsCl}-C'_{AlCl_3}$/M	$-\log (C'_{CsCl}-C'_{AlCl_3})$
T1−2[b]	0.4632_1	57.6	0.4312	1.0017_5	-0.0007_6
T1−3[b]	0.4370_3	19.3	0.1445	1.7393_4	-0.2403_8
T1−4[b]	0.4321_6	14.2	0.1063	1.8787_8	-0.2738_8
T1−5[b]	0.4256_6	8.18	0.0612	2.0659_0	-0.3151_2
S3−2[c]	0.4645_3	75.44	0.3990	0.9651_7	-0.01539_6
S3−3[c]	0.4544_9	53.90	0.2937	1.2450_5	-0.0951_9
S3−4[c]	0.4441_7	35.58	0.1928	1.5362_0	-0.1864_4
S3−5[c]	0.4332_3	18.33	0.1029	1.8477_4	-0.2666_4
R1−3[c]	0.4604_2	63.97	0.3492	1.0793_3	-0.0331_6
T3−3[b]	0.5291_0	852.7			
T3−4[b]	0.5200_2	825.6			
T3−5[b]	0.5151_8	806.1			
T3−6[b]	0.5065_0	750.3			
R1−2[c]	0.5216_5	829.6			

[a]Determined from weights. [b]Chlorine/chloride type cell, $Y = -F\Delta E_{Cl}/RT \ln 10$. [c]Chloroaluminate/aluminium type cell, $Y = -3F/4RT \ln 10\ [\Delta E_{Al} - RT/3F \ln ([AlCl_4^-]_{ref}/[AlCl_4^-])]$.

in Fig. 5 gives a straight line through the origin with a slope of 45±3 °C kg mol^{-1}. This slope is much influenced by the θ values at high *m*, and seems to be too low for the limiting λ. An alternative way of obtaining λ is to plot θ/*m* against *m* as shown in Fig. 6, whereupon λ is determined

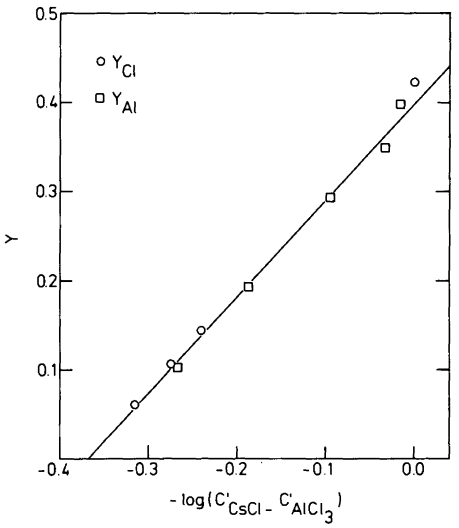

Fig. 7. Potentiometrically determined *Y*, eqns. (8, 9), plotted versus the logarithm of the difference in pre-reaction concentrations of CsCl and $AlCl_3$, used to determine pCl_{ref} in basic CsCl/$AlCl_3$ melts at 400 °C.

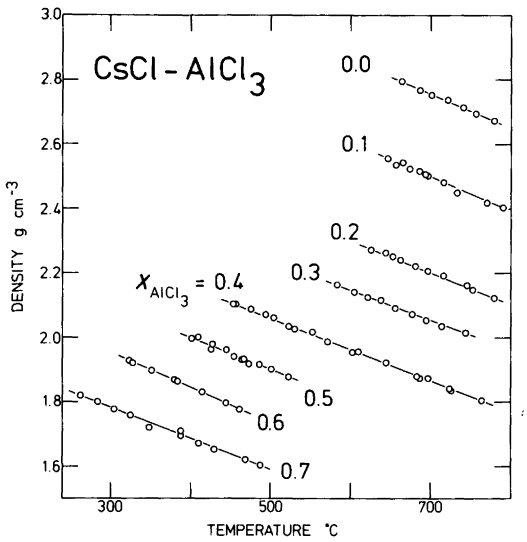

Fig. 8. Density ϱ of CsCl/$AlCl_3$ melts vs. temperature *T* and composition(mole fraction x_{AlCl_3}).

as the intercept at $m = 0$. Linear regression of the θ/m data in Fig. 6 gives an intercept of 78±6 °C kg mol^{-1}. Omission of the high *m* points gives even larger values of λ. It was finally concluded that the best estimate for λ is 75±25 °C kg mol^{-1}.

Enthalpy and entropy of fusion for $CsAlCl_4$. The λ value can be used for obtaining the enthalpy of fusion, ΔH_f, at the melting point (660.9 K), using eqn. (5). The result is ~15 kJ mol^{-1}, the estimated uncertainty range being from 11–23 kJ mol^{-1}. No calorimetric value exists in the literature, but the value is close to those found for $NaAlCl_4$ and $KAlCl_4$ (15.5 and 18.0 kJ mol^{-1}).[1,2] The entropy of fusion, ΔS_f, of $CsAlCl_4$, calculated as $\Delta H_f/T_f$, is ~23 J mol^{-1} K^{-1}, the estimated uncertainty range being from 16–33 J mol^{-1} K^{-1}. This seems reasonable in view of the values found for $NaAlCl_4$ and $KAlCl_4$ (36.1 and 33.9 J mol^{-1} K^{-1}).[1,2]

Potentiometry. The electrochemical cell (Fig. 3) had two separate compartments with CsCl/$AlCl_3$ melts, one of which (the reference) was saturated with CsCl crystals at the appropriate temperature (400 °C). The weights of $AlCl_3$ were not corrected

Table 5. Potentiometrically determined p*K* values and variances for different models of the CsCl/$AlCl_3$ system at 400 °C.

Model No.	Equilibria	Constant	Obtained p*K* value	Variance
1	$2AlCl_4^- \rightleftharpoons Al_2Cl_7^- + Cl^-$	K_1	7.627(4)	$1.12 \cdot 10^{-7}$
2	$2AlCl_4^- \rightleftharpoons Al_2Cl_7^- + Cl^-$ $Al_2Cl_7^- \rightleftharpoons Al_2Cl_6 + Cl^-$	K_1 K_2	7.65(1) 7.6(2)	$4.19 \cdot 10^{-8}$
3	$2AlCl_4^- \rightleftharpoons Al_2Cl_7^- + Cl^-$ $3Al_2Cl_7^- \rightleftharpoons 2Al_3Cl_{10}^- + Cl^-$	K_1 K_3	7.65(1) 8.7(5)	$4.17 \cdot 10^{-8}$

Table 6. Density of $CsCl/AlCl_3$ mixtures. Results of least-squares linear regression fitting of an equation $\varrho(x_{AlCl_3}) = A - B \cdot 10^3 \cdot T$ to the density data (available from authors).[a]

x_{AlCl_3}	No. of points	Range in T/ °C	A/ g cm^{-3}	B/ g cm^{-3} °C^{-1}	Model SD/ g cm^{-3}	R^2
0.7000	11	262–466	2.0699(99)	0.965(26)	0.0061	0.99343
0.6000	8	321–459	2.2664(53)	1.055(13)	0.0019	0.99899
0.5000	12	399–521	2.4054(259)	1.015(57)	0.0069	0.96968
0.4000	18	453–762	2.5571(63)	0.992(11)	0.0044	0.99821
0.3000	9	582–743	2.7193(163)	0.956(25)	0.0037	0.99535
0.2000	11	624–778	2.9006(132)	0.998(19)	0.0033	0.99682
0.1000	13	644–788	3.2668(284)	1.105(40)	0.0064	0.98580
0.0000	8	661–777	3.4729(167)	1.028(23)	0.0026	0.99701

[a] ϱ is the density in g cm^{-3}. T is the temperature in °C. SD is the crude standard deviation of the model fit to the data, without taking into account the precision of ϱ and T (the true SD is larger).

for unavoidable but small AlOCl content. The experimental cell voltages are reported in Table 4 as a function of the composition of the melt. The interpretation of the potentiometric data is analogous to that given in previous work;[3,4] molar equilibrium concentrations, symbolized by [ ] in mol l^{-1} of melt, and pre-reaction total concentrations, C′, specifying the initial molarity, were calculated using the density expression [eqn. (12)].

It can be shown[17] that the cell voltage (ΔE) of the concentration cell will be given approximately by the Nernst expressions, eqns. (6) and (7), for chlorine/chloride and chloroaluminate/aluminium electrodes, respectively.

$$\Delta E_{Cl} = -\frac{RT}{F} \ln ([Cl^-]_{ref}/[Cl^-]) \quad (6)$$

$$\Delta E_{Al} = -\frac{4RT}{3F} \ln ([Cl^-]_{ref}/[Cl^-]) + \frac{RT}{3F} \ln ([AlCl_4^-]_{ref}/[AlCl_4^-]) \quad (7)$$

The accuracy of these equations is unknown in the present case; no transference numbers nor activity coefficients are known for the $CsCl/AlCl_3$ system. By assuming the mobilities of the ions involved to be inversely proportional to their ionic radii,[17] it is possible to show that the error related to the transference numbers is probably about 5 mV for the most extreme case (852.7 mV). Rearranging eqns. (6) or (7) and using the definition $pCl = -\log[Cl^-]$, the pCl of the sample melt can be expressed in terms of known quantities and pCl_{ref}, the pCl of the CsCl-saturated reference.

Solubility of solid CsCl in $CsAlCl_4$ at 400 °C. In basic $CsCl/AlCl_3$ melts (except those very close to the 1:1 composition), the only complex present is $AlCl_4^-$. The excess of CsCl therefore gives rise to a corresponding amount of chloride ion and the pCl will be equal to $-\log(C'_{CsCl} - C'_{AlCl_3})$. Hence, a plot of eqn. (8) or eqn. (9) versus $-\log(C'_{CsCl} - C'_{AlCl_3})$ should give a straight line having a slope of unity and an intercept at the abscissa ($\Delta E = 0$) corresponding to pCl_{ref} at the temperature in question.

$$Y_{Cl} = -\Delta E_{Cl} (F/RT \ln 10) \quad (8)$$

$$Y_{Al} = -(\Delta E_{Al} - (RT/3F) \ln ([AlCl_4^-]_{ref}/[AlCl_4^-])) \cdot (3F/4RT \ln 10) \quad (9)$$

Such a plot, based on our 9 basic samples at 400 °C, is shown in Fig. 7. The $AlCl_4^-$ reference concentration needed for the evaluation of Y_{Al} (the 5 points corresponding to ΔE_{Al} measurements) was obtained iteratively, starting from assumed identical $AlCl_4^-$ concentrations in sample and reference melts.

The straight line in Fig. 7 is a least-squares regression line through the nine points, giving a slope of 1.08±0.04 and a coefficient of determination[19] of $R^2 = 0.9891$. Extrapolation to the abscissa gives $pCl_{ref} = -0.37 \pm 0.02$. Omission of the two points with the highest Y values (initial meas-

urements on melts, perhaps not in equilibrium due to slow dissolution of CsCl in the reference, and experiments where the previously mentioned assumptions are most unrealistic) changes the slope to 1.035±0.022 and gives pCl_{ref} = −0.375±0.010. Knowing now the saturation concentration of CsCl, the density as a function of composition [see eqn. (12)], and the C'_{CsCl} and C'_{AlCl_3} values at 400 °C, we can by iteration calculate x_{AlCl_3} at saturation to be 0.4151, the value used previously in evaluation of the phase diagram (Fig. 4). Also, we obtain $[Cs^+]_{ref}$ = 8.17 mol l^{-1} and a stoichiometric solubility product for CsCl, $K_s = [Cs^+] \cdot [Cl^-]$ = 19.38 $mol^2\ l^{-2}$ at 400 °C. Comparing this value to analogous values for the corresponding sodium and potassium systems,[2] we see that CsCl has the highest solubility among the three MCl/$AlCl_3$ systems, even when the higher temperature is taken into consideration.

Model equilibria for the non-basic CsCl/$AlCl_3$ melts. The free chloride concentration as a function of melt composition for melts having near-neutral or acidic composition (Table 4) can be obtained using eqns. (6) and (7), once the saturation concentration of CsCl has been determined. The five bottom pCl values, and the corresponding melt compositions (Table 4) were used as input data to a model-fitting algorithm which, from guessed sets of model equilibria and associated equilibria constants, calculated model x_{AlCl_3} values corresponding to the pCl number and then optimized the constants. As a result, best possible fits to sets of supposed model equilibria and corresponding concentration equilibrium constants were obtained as shown in Table 5. When compared with previous data for pK values (Table 1), a satisfactory consistency is observed.

Density of CsCl/$AlCl_3$ melts. The experimental densities, measured for eight compositions, are plotted versus temperature in Fig. 8. (The numerical density data are available from the authors upon request). As can be seen, for each composition there is a largely linear dependence on temperature. These data were used in a least-squares fitting procedure to determine the parameters A and B in the density expression given by eqn. (10) where ϱ = density in g cm^{-3} and T = temperature in °C.

$$\varrho = A - B \cdot 10^{-3} \cdot T \qquad (10)$$

The obtained A and B parameters are given in Table 6. In prior literature,[22–24] density expressions are given only for the compounds CsCl and $CsAlCl_4$. It is interesting to note the concordance between these expressions and ours: for CsCl, Janz *et al.*[22] summarized previous investigations in recommending the expression ϱ_{CsCl} = 3.4783–$1.0650 \cdot 10^{-3} \cdot T$, obtained by Yaffe and van Artsdalen[23] in the range 670–905 °C (standard deviation of model = 0.0006 g cm^{-3}); for $CsAlCl_4$, Brynestad[24] obtained the expression ϱ_{CsAlCl_4} = $2.403–1.010 \cdot 10^{-3} \cdot T$. Both of these equations are, within error limits, identical to our results.

All density data in Fig. 8 may be conveniently represented by one empirical equation. Using a standard least-squares regression method, we obtained the most satisfactory simple polynomial expression (11) for A = 2.407(13), B = −0.001000(25), C = 1.545(25), D = 2.29(9); standard deviation = 0.016 g cm^{-3} (better than 1 %); R^2 = 0.9973 (g cm^{-3} and °C units). Analytical expressions with higher order terms like T^2 or $T \cdot x$ or x^2, etc. were not found useful.

$$\varrho = A + BT + C(0.5 - x_{AlCl_3}) + D(0.5 - x_{AlCl_3})^3 \qquad (11)$$

For calculations of the density of CsCl/$AlCl_3$ mixtures at 400 °C, the more accurate expression eqn. (12) can be used, with A = 2.823(7) g cm^{-3} and B = 1.623(15) g cm^{-3}; model standard deviation of 0.007 g cm^{-3}; R^2 = 0.9995. This equation was obtained by calculating the density at 400 °C from the model data in Table 6 and then fitting a regression line, eqn. (12), to the points for different x_{AlCl_3}.

$$\varrho = A - B \cdot x_{AlCl_3} \qquad (12)$$

Container corrosion for glass cells. It was observed that the freezing point of some melts increased when the samples were held molten for several days. In particular, this was found for melts of acidic composition (Table 2, expts. E–O and G–O) and also to some extent for basic melts (expts. F–O H–O and B–4), whereas samples of neutral compositions had more stable freezing points. Also, the cell potentials varied with time; however, this could be due to diffusion through the separator. We assumed that the lack of stability was due to corrosion of the glass. Glass surfaces looked much etched (milky and

Table 7. Corrosion experiments with $CsCl/AlCl_3$ in Pyrex tubes during one week of rocking at 400 °C.

x_{AlCl_3}	Average loss per piece/g	Condition visually	Liq.-N_2-condensable gas present
Pyrex[a]			
0.4790	0.0005(6)[b]	unchanged	traces
0.5017	0.0001(1)	melt unchanged or with faintly black particles	no
0.5245	0.0013(2)	glass milky and etched	yes
Steel[c]			
0.4790	0.00008(5)[d]	metal extra shiny	no
	0.00025(6)[e]	melt faintly pink	
0.5002	0.00005(6)[d]	unchanged	no
	0.00028(13)[e]	melt faintly yellow	
0.5197	0.00002(2)[d]	metal rusty,	traces
	0.0029(8)[e]	corroded; black deposits on glass melt unchanged	

[a]Each cell contained 3 pieces of Pyrex tubing, each ca. 1.3 g, surface ~0.8 cm^3. [b]One glass piece carried all the corrosion because of insufficient wetting. [c]Each Pyrex cell contained 3 pieces of the two steels, each ~0.5 g, surface ~1 cm^3. [d]Kovar steel (29 Ni, 17 Co, 0.2 Si, 0.3 Mn, 0.02 C). [e]NU 3L stainless Steel (18.5 Cr, 9.5 Ni, max. 0.030 C).

semi-transparent) after contact with acidic melts for weeks. On cooling unopened cells in liquid nitrogen, a gas could be condensed as a liquid/solid in relatively large quantities for acidic samples, to some extent for basic samples, and in trace amounts for near neutral samples (no condensable gas was seen before the first melting of the reagents). The condensable gas in the case of experiments E–O was found to be $SiCl_4$ by means of its gas-phase spectrum (Raman bands at 425 (strong), 220 (medium) and 150 (medium) cm^{-1}). For technical details, see e.g. Ref. 25.

The formation of $SiCl_4$ has previously been observed when $AlCl_3$ reacted with quartz at temperatures over 300 °C.[26] We therefore examined to some extent this glass corrosion. A number of 10–20 mm long, carefully cleaned and weighed pieces of borosilicate glass tube were placed inside three cells to which reagents were added in amounts such that the compositions were basic neutral or acidic, respectively. After melting and one week of rocking at 400 °C, the glass pieces were taken out, rinsed in water, and examined by weighing and inspection (Table 7). The glass which had been in contact with the 52 % $AlCl_3$ acidic melt was clearly etched and also looked corroded. The experiment in basic melt gave indication of weight losses. Glass subjected to the neutral melt seemed unchanged. The observations can be explained by assuming the following corrosion reactions to occur in acidic [eqn. (13)] or basic [eqn. (14)], environments:

$$2AlCl_3 + SiO_2(s) \rightarrow \frac{2}{n}(AlOCl)_n + SiCl_4 \qquad (13)$$

$$4CsCl + 2SiO_2(s) \rightarrow \frac{1}{m}(Cs_4SiO_4)_m + SiCl_4 \qquad (14)$$

The compositions calculated, *when not corrected for these reactions*, are thus either less acidic [eqn. (13)] or less basic [eqn. (14)]. Hence, the melt should be more neutral and thus higher melting than a calculation starting from the weights of CsCl and $AlCl_3$ would predict. Impurities formed by the corrosion may depress the freezing point, but since they probably tend to go into the gas phase ($SiCl_4$), or to be large, polymeric species [$(AlOCl)_n$ and $(Cs_4SiO_4)_m$], the effects of these impurities are not expected to override the elevating tendency due to the neutralization action of the corrosion processes. In this way, it is understood why it is only in the uncorrosive near neutral melts that our results (see Fig. 4) are higher than those of the literature. In more acidic or basic melts the corrosion is fast, and the clean starting melts are quickly contaminated.

Container corrosion for stainless steel cells. We also examined the corrosion of the stainless steel used for construction of the metallic containers. Pieces of carefully cleaned and weighed NU 3L steel and Kovar steel [used for the lids only (Fig. 2)] were placed inside evacuated glass cells containing basic, neutral or acidic $CsCl/AlCl_3$ mixtures. After melting and one week of rocking at 400 °C, the metallic pieces were taken out, rinsed in water and examined (Table 7). The NU 3L steel lost weight in all three cases, but most notably in the acidic melt. Kovar steel apparently has a much better corrosion resistance, but unfor-

tunately it was not possible to obtain all-Kovar steel containers.

Conclusions

The data reported in the present paper are reproducible and in relatively good agreement with previous results. However, it must be emphasized that all results obtained in glass or stainless steel containers should be considered inaccurate due to the unavoidable corrosion reactions. The presence of oxides as impurities in basic, neutral, and acidic CsCl/AlCl$_3$ melts can be conveniently detected by infrared and Raman spectroscopy, as shown recently.[25]

Acknowledgements. We are grateful for help from G. N. Papatheodorou, B. M. Faanes and S. von Winbush, for equipment grants from *Thomas B. Thriges Fond, Danmarks Tekniske Højskoles Fond for Teknisk Kemi, Julie Damms Studiefond* and The Ministry of Energy (Denmark).
One of us (T.Ø.) received support from the Technical University of Denmark, from the Norwegian Research Foundations NAVF and NTNF and from *Fondet for Dansk-Norsk Samarbejde.*

References

1. Berg, R. W., Hjuler, H. A. and Bjerrum, N. J. *Inorg. Chem. 23* (1984) 557.
2. Berg, R. W., Hjuler, H. A. and Bjerrum, N. J. *Inorg. Chem. 24* (1985) 4506.
3. Brekke, P. B., von Barner, J. H. and Bjerrum, N. J. *Inorg. Chem. 18* (1979) 1372.
4. Hjuler, H. A., Mahan, A., von Barner, J. H. and Bjerrum, N. J. *Inorg. Chem. 21* (1982) 402.
5. Morozov, I. S. and Simonich, A. T. *Russ. J. Inorg. Chem. 2* (1957) 311.
6. van der Kamp, L. K. and van Spronsen, J. W. *Z. Anorg. Allg. Chem. 361* (1968) 328.
7. Pöyhönen, J. and Ruuskanen, A. *Ann. Acad. Sci. Fenn. Ser. A VI, 146* (1964) 1.
8. Stull, R. D. and Prophet, H. *JANAF Thermochemical Tables, Natl. Stand. Ref. Data Ser. 37, Natl. Bur. Stand. (US)* 1971, pp. ClCs.
9. Fannin, A. A., King, L. A., Seegmiller, D. W. and Øye, H. A. *J. Chem. Eng. Data 27* (1982) 114; Carpio, R. A., Fannin, A. A., Kibler, F. C., King, L. A. and Øye, H. A. *J. Chem. Eng. Data 28* (1983) 34.
10. Torsi, G. and Mamantov, G. *Inorg. Chem. 11* (1972) 1439.
11. Schulze, K., Steinle, D. and Hoff, H. *Z. Naturforsch., Teil A 28* (1973) 1847.
12. Ikeuchi, H. and Krohn, C. *Acta Chem. Scand., Ser. A 28* (1974) 48.
13. Berg, R. W., von Winbush, S. and Bjerrum, N. J. *Inorg. Chem. 19* (1980) 26.
14. Øye, H. A. and Wahnsiedler, W. E. In: Blander, M. *et al.*, Eds., *Proc. 4th Int. Symp. on Molten Salts.* The Electrochemical Society, Pennington N. J. 1984, p. 274.
15. Grande, K., Hertzberg, T. and Øye, H. A. *Light Metals 115th Annual Meeting,* New Orleans, March 2–6, 1986. Vol. 2, p. 431.
16. Wærnes, O., Palmisano, F. and Østvold, T. *Acta Chem. Scand., Ser. A 37* (1983) 207.
17. von Barner, J. H. and Bjerrum, N. J. *Inorg. Chem. 12* (1973) 1891.
18. Berndt, A. F. and Diestler, D. J. *J. Phys. Chem. 72* (1968) 2263.
19. Coefficient of determination for a model $y = f(x)$ is defined as $R^2 = [\Sigma(x-\bar{x})\,(y-\bar{y})]^2/[\Sigma(x-\bar{x})^2\Sigma(y-\bar{y})^2]$ where $\bar{x} = \Sigma x/n$ and n = number of points (x,y).
20. Brynestad, J. *Z. Phys. Chem. NF 30* (1961) 123.
21. Zachariassen, K., Berg, R. W., Bjerrum, N. J. and von Barner, J. H. *J. Electrochem. Soc. In press.*
22. Janz, G. J., Dampier, F. W., Lakshminarayanan, G. R., Lorenz, P. K. and Tomkins, R. P. T. In: *Molten Salts, Electrical Conductance, Density and Viscosity Data, Vol. 1, Natl. Stand. Ref. Data Ser. 15, Natl. Bur. Stand. (US),* Washington, D.C. 1968, pp. 1–139.
23. Yaffe, I. S., and van Artsdalen, E. R. *J. Phys. Chem. 60* (1956) 1125.
24. Brynestad, J. Oak Ridge National Laboratory, *Personal communication* (unpublished).
25. Berg, R. W. and Østvold, T. *Acta Chem. Scand., Ser. A 40* (1986) 445.
26. Schäfer, H., Trenkel, M. and Peine, M. *Z. Anorg. Allg. Chem. 445* (1978) 129.

Received May 27, 1986.